IEEE Access
Multidisciplinary | Rapid Review | Open Access Journal

Received July 17, 2019, accepted August 2, 2019, date of publication August 13, 2019, date of current version September 17, 2019.

Digital Object Identifier 10.1109/ACCESS.2019.2935034

Improved Measurement of the Low-Frequency Complex Permeability of Ferrite Annulus for Low-Noise Magnetic Shielding

KE YANG[1], JIXI LU[1,2], MING DING[1,2,3], JUNPENG ZHAO[1], DANYUE MA[1], YANG LI[1], BOZHENG XING[1], BANGCHENG HAN[1,2,3], AND JIANCHENG FANG[1,2]

[1]School of Instrumentation and Optoelectronic Engineering, Beihang University, Beijing 100191, China
[2]Zhejiang Laboratory, Hangzhou 311121, China
[3]Hangzhou Innovation Institute, Beihang University, Hangzhou 310051, China

Corresponding author: Jixi Lu (lujixi@buaa.edu.cn)

This work was supported in part by the Natural Science Foundation of Beijing Municipality under Grant 4191002, in part by the National Natural Science Foundation of China under Grant 61903013, and in part by the National Key R&D Program of China under Grant 2017YFB0503100.

ABSTRACT The ferrite magnetic shield can provide a low-noise magnetic environment for various ultrahigh-sensitivity measurements. The low-frequency complex permeability, which determines the magnetic hysteresis noise and the shielding factor, is a key parameter of the ferrite shield and thus should be measured accurately. In this paper, the measurement error of conventional coil method is analyzed at low frequency, and an improved method is proposed which could eliminate the measurement error introduced by the wire resistance. Using this method, four ferrite samples made of PC40 and PC47 materials are measured. The measurement accuracy of the low-frequency complex permeability has improved by two orders of magnitude. On the basis of the measurement results, magnetic hysteresis noise and the shielding factor of ferrite shields are calculated. The calculated results of the noise analysis indicate that the PC40 material has lower magnetic hysteresis noise. This study can help select the ferrite materials and estimate the performance for low-noise magnetic shield design.

INDEX TERMS Permeability measurement, ferrites, magnetic noise, magnetic shielding.

I. INTRODUCTION

In modern physics, various sensitive measurements rely on high-performance magnetic shields to reduce interference by the external magnetic field [1]. In addition to the shielding factor, which characterizes the attenuation degree of external magnetic field, the magnetic noise generated by the magnetic shield is a key parameter which determines the limitation of the ultrahigh-sensitivity measurements [2]. For example, the sensitivity of some ultrahigh-sensitivity atomic magnetometers is limited by the magnetic noise generated by the innermost layer of the magnetic shield itself [3], [4]. For conventional magnetic shields made of high-permeability metals (eg. μ-metal), the intrinsic magnetic noise is limited to 1–10 $fT \cdot Hz^{-1/2}$ by eddy-current noise due to low electrical resistivity. The ferrite with high permeability and high electrical resistivity is an ideal material for magnetic shields due to it has both high shielding factor and low magnetic noise. T. Kornack *et al.* developed a Mn-Zn ferrite shield and demonstrated that a spin-exchange relaxation-free (SERF) atomic magnetometer with it achieved a sensitivity of $0.75\,fT \cdot Hz^{-1/2}$ at 35–200 Hz [5]. This sensitivity is 25 times better than what would be expected in a μ-metal shield with a comparable size. Since then ferrite shields have been widely used in high-precision measurement such as instrumentations for low-field nuclear magnetic resonance (NMR) [6], nuclear magnetic resonance gyroscopes (NMRGs) [7], atomic magnetometers [5], [8], [9] and co-magnetometers [10].

At low frequency, the magnetic hysteresis noise determined by the complex permeability dominates the magnetic noise of ferrite shields rather than the magnetic eddy-current noise [2], [5]. In addition to the magnetic hysteresis noise, the shielding factor of the magnetic shield at the low frequency is determined by the low-frequency complex permeability [11], [12], which is also an important material parameter for ferrite shields. Further, the permeability of ferrites made of different components or from different batches usually show a large variation. Therefore, the

The associate editor coordinating the review of this article and approving it for publication was Bora Onat.

 This work is licensed under a Creative Commons Attribution 4.0 License. For more information, see http://creativecommons.org/licenses/by/4.0/

accurate measurement of the low-frequency complex permeability of actual ferrite shields is important, which could help estimate both the magnetic noise and the shielding factor of the ferrite shield at low frequency accurately and suggest shield materials.

There are three kinds of conventional methods to measure the complex permeability which mainly focus on high frequency. The first is the ''transmission method'' [13]–[17], by means of the variation of the reflected and transmitted field. The measurement sensitivity drops rapidly with the decrease of the frequency due to the decreased transmission and reflection field energy at a lower frequency. This method is usually used for planar samples or wires, and not suitable for toroidal samples. The second is the ''coaxial line method'' [18]–[22]. The complex permeability of the toroidal ferrite sample can be measured using an impedance analyzer or a network analyzer with the coaxial line technique for frequency above 1 kHz. In this case, the size of the sample is usually limited to be smaller than 20 mm due to the size of the coaxial line device. The device allows for the ideal structure, configuring a single-turn inductor with the sample. However, due to the equivalent turns, the impedance of the single-turn inductor is too small to be measured precisely below 1 kHz. The third is the ''coil method'' [5], [23], [24]. The complex permeability is derived from the inductance and resistance of the toroidal coil wound around the ferrite sample. Because there are more coil turns, the coil method can produce bigger impedances to measure than the coaxial line method. However, at low frequency, there is a measurement error for the imaginary permeability due to the wire resistance. This error has a significant impact on the determination of the imaginary permeability at the low frequency range — see Section II.

In this paper, we propose an improved coil method to measure the low-frequency complex permeability of the ferrite annulus for low-noise magnetic shields. The measurement error of the conventional coil method is investigated. The analysis indicates that the resistance of the wire is the primary cause affecting the measurement at low frequency. In the improved method, the wire resistance is separated from the measured resistance using the linear fitting method, which eliminates the measurement error of the imaginary permeability at low frequency. The experimental results indicate that the improved method can effectively reduce the low-frequency measurement error. In addition, the magnetic noise and the shielding factor of ferrite shields, which are developed using the PC40 and PC47 ferrites, are calculated using the obtained complex permeability.

II. PRINCIPLES

Magnetic permeability usually cannot be measured directly, but can be transformed into electronic parameters to measure by winding coils around the toroidal ferrite sample. The distributed capacitance of the coils is very small and can be ignored, and the equivalent resistance is much smaller than the equivalent reactance at low frequency.

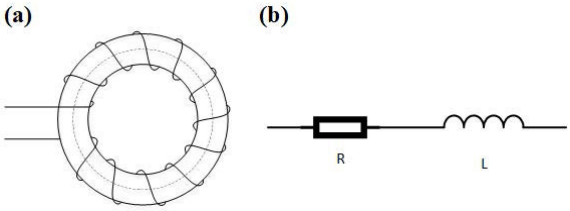

FIGURE 1. (a) The schematic diagram of coil around a toroidal ferrite sample (not to scale). (b) Equivalent series circuit.

The coils wound around the ferrite core are equivalent to a resistance-inductance series circuit – see Fig. 1.

Using the equivalent series circuit, the relationship between the inductance L_s and resistance R_s of the windings and the complex permeability can be described by [24]

$$\mu' = \frac{l_e}{\mu_0 A_e N^2} L_s \tag{1}$$

$$\mu'' = \frac{l_e}{\mu_0 A_e N^2 \omega} R_s \tag{2}$$

where L_s and R_s are the inductance and resistance of the equivalent series circuit, A_e is the equivalent cross-section area of the ferrite sample, N is the number of turns of the coils, l_e is the equivalent length of the magnetic path, $\omega = 2\pi f$ is the angular frequency of the driving field, μ_0 is the permeability of vacuum, μ' and μ'' are the real part and imaginary part of the relative complex permeability respectively.

On the basis of the measured inductance and resistance of the equivalent circuit, the real part and imaginary part of the complex permeability can be acquired. In the experiment, the series resistance can be obtained using a LCR meter. It contains not only R_s but also the wire resistance. Hence, the resistance obtained from the LCR meter can be formulated as

$$R_s^{LCR} = R_s + R_w \tag{3}$$

where R_s^{LCR} is the series resistance obtained from the LCR meter, and R_w is the resistance of the wire. The wire resistance R_w contains the wire resistance of the coil R_{wc}, the resistance of the probe wire R_p, and the contact resistance between the probe and coil R_c. R_{wc} is the primary part of R_w.

To study the influence of R_w, a theoretical analysis is made below. In this experiment, the length of the copper enameled wire used for the measurement coil is about 1500 mm and the diameter is 0.71 mm. And thus R_{wc} is about 65.16 mΩ. R_w is estimated to be about 70 mΩ. μ'' and R_w stay constant over the small frequency range we measured. μ'' is generally within the range of 1 to 500 for a wide frequency-band [20]. Here, to be more visualized, μ'' is assumed to be 50. Fig. 2 shows the comparison between the calculated R_s and R_w as a function of the frequency and the percentage of R_w with respect to R_s^{LCR} at different frequencies.

According to the analysis result, R_w takes up a significant part of R_s^{LCR} at low frequency and cannot be neglected.

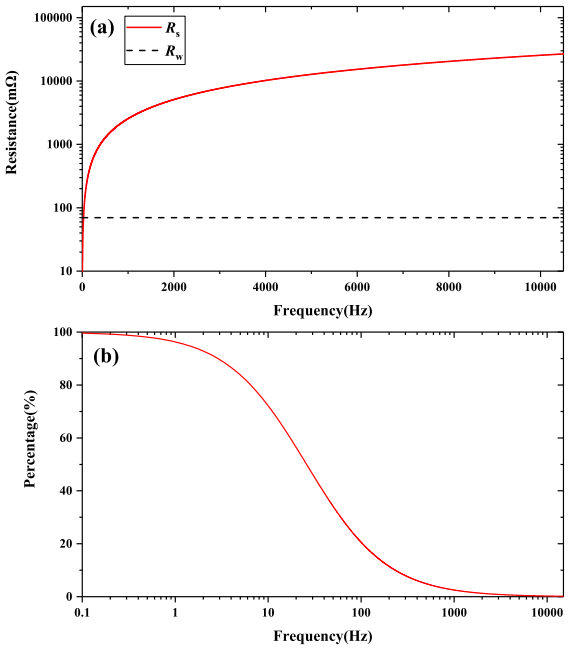

FIGURE 2. (a) Comparison between the calculated R_S and R_W as a function of frequency; (b) Percentage of the calculated R_W with the respect to R_S^{LCR}.(R_W is estimated to be about 70 mΩ; $R_s = \mu_0 A_e N^2 \omega \mu'' / l_e$; $R_S^{LCR} = R_s + R_W$.)

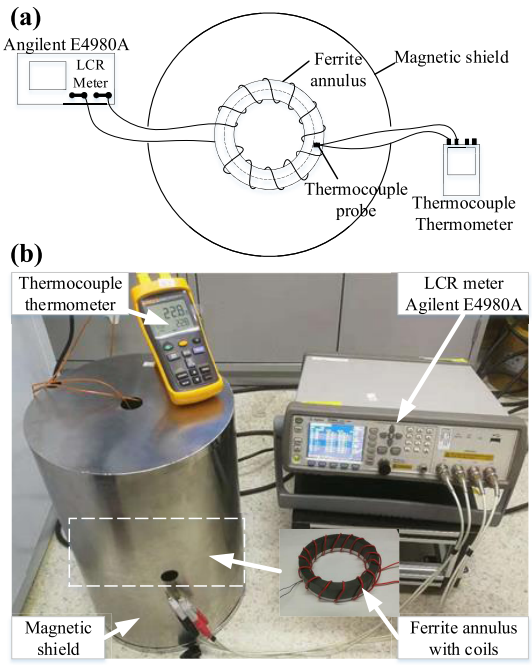

FIGURE 3. The experimental setup to measure the low-frequency complex permeability of the ferrite annulus. (a) Schematic diagram (not to scale). (b) Photograph.

However, R_s can reach 100 Ω or even $k\Omega$ at the higher frequency and much larger than R_w. Therefore, R_w is relatively small and usually ignored at high frequency. If R_s^{LCR} is used directly instead of R_s to calculate the imaginary permeability according to (2) at low frequency, it would cause a significant measurement error for the imaginary permeability. To obtain the accurate imaginary permeability, R_w needs to be identified and eliminated.

To obtain R_w, (3) can be rewritten as

$$R_s^{LCR} = A \cdot f + R_w \tag{4}$$

where $A = 2\pi\mu_0 A_e N^2 \mu'' / l_e$ is a constant. Therefore, the obtained R_s^{LCR} can be fitted to (4) using the linear fitting for deriving R_w and A. Accordingly, the measurement error of the imaginary permeability from the wire resistance can be eliminated and a more accurate permeability can be obtained.

The obtained complex permeability is the amplitude permeability due to the driving field. In the magnetic shield system, the ferrite shield is usually located at the innermost layer of shield where the magnetic field is near zero. Therefore, the complex permeability used to calculate the magnetic noise and shielding factor should be the initial complex permeability which is limited to the zero driving field. The extrapolation method is used to obtain the initial complex permeability from the amplitude permeability. When the driving field is small enough, the initial complex permeability can be linked with the amplitude permeability using the Rayleigh relation [24], which is described by

$$\mu_a = \mu_i + \eta \hat{H} \tag{5}$$

where μ_a is the amplitude permeability, μ_i is the initial complex permeability, η is the Rayleigh constant, and $\hat{H}$ is the maximum value of the driving magnetic field strength. According to (5), we could extrapolate the complex permeability to the zero field to obtain the initial permeability by fitting the permeability field response function to (5).

III. EXPERIMENT

A. EXPERIMENTAL SETUP

The experimental setup is shown in Fig. 3. A ferrite sample, surrounded by a 16-turn measurement coil, is placed in a one-layer μ-metal magnetic shield. Besides, the demagnetization coils are also wound around the ferrite for demagnetizing. Before every measurement, the ferrite annulus sample was demagnetized, which can keep the magnetization of samples same and zeroed and eliminate the influence of magnetization. The inner magnetic field in the magnetic shield is measured by a fluxgate magnetometer. The μ-metal magnetic shield is able to shield the external magnetic field to be about 100 nT. The seams and orifices of the magnetic shield will not make a significant impact on our measurement. The used μ-metal is Nickel-Iron soft magnetic alloys. The diameter, the thickness and the length of the μ-metal magnetic shield are 28 cm, 2 mm and 42 cm respectively. There are four ferrite samples measured in this work. The first three are made of Mn-Zn ferrite PC40 material from TDK Corporation with different dimensions. The fourth ferrite sample measured are made of Mn-Zn ferrite PC47 materials from TDK Corporation. Their dimensions are shown as Table 1. The nominal value of initial relative permeability of PC40 and PC47 materials are 2300 at 23 °C under the field strength 0.4 A/m and

TABLE 1. The materials and dimensions of the ferrite samples.

Sample number	Material	Outside diameter (mm)	Height (mm)	Inside diameter (mm)
Sample 1	PC40	133	25	108
Sample 2	PC40	96	20	70
Sample 3	PC40	80	20	50
Sample 4	PC47	133	25	108

$2500 \pm 25\%$ respectively from 1 kHz to 200 kHz according to the product manual [25]. An LCR meter (Agilent E4980A) is used to measure both the inductance and the resistance of the windings via the hole in the middle of the magnetic shield. The driving current of the LCR meter can be set using the panel and is accurately shown on the screen of LCR meter. The frequency range of the LCR meter is from 20 Hz to 2 MHz. A thermocouple thermometer is used to monitor the temperature whose probe is attached to the ferrite sample. Because the temperature significantly affects the results, all measurements were performed under controlled temperature conditions.

B. EXPERIMENTAL PROCEDURE

First of all, a copper enameled wire was wound around the annulus sample as the measurement coil. A silver plated copper wire was wound around the annulus sample as the demagnetization coil. The ferrite annulus was placed at the center of the magnetic shield. Before the measurement, the ferrite samples were demagnetized using AC demagnetization method [26], [27]. The driving current of the LCR meter I was applied to the measurement coil and the corresponded driving magnetic field strength was H. The L_s and R_s^{LCR} of the measurement coil were measured at the frequency range from 20 Hz to 2 MHz by the LCR meter. According to (1), the real part of permeability can be obtained easily from L_s. R_s^{LCR} was linearly fitted to (4) from 20 Hz to 200 Hz, and the wire resistance R_w was obtained at the driving field strength H. Hence, R_s was obtained by eliminating R_w from R_s^{LCR} according to (3). The imaginary part of permeability after correction was obtained according to (2). The complex permeability were obtained under the driving field strength H after eliminating the measurement error. Then, the driving current of the LCR meter was increased to increase the field strength from 0.40 A/m to 1.10 A/m by step. The low-frequency complex permeability (20Hz–200Hz) under the different driving field were obtained after eliminating the measurement error. The measurement was operated for 10 times at each frequency and the multiple measurements were averaged. Finally, the complex permeability was extrapolated to the zero field to derive the initial permeability, by fitting the permeability field response function to (5).

C. RESULTS AND DISCUSSION

R_w was separated from the measured resistance R_s^{LCR} as measurement error using the linear fitting with (4). The fitting results are shown in Fig. 4. The fittings results indicate the wire resistances of 65.94 mΩ for Sample 1, 60.52 mΩ for Sample 2, 65.15 mΩ for Sample 3 and 66.48 mΩ for Sample 4.

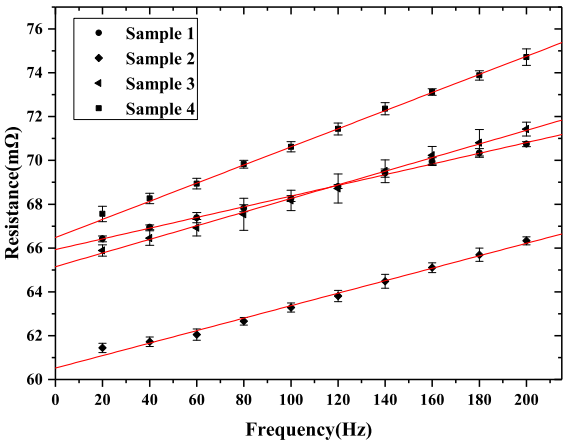

FIGURE 4. The experimentally obtained resistances of Sample 1 (black circles), Sample 2 (black rhombus), Sample 3 (black triangle) and Sample 4 (black squares) were fitted to (4) (red line). The error bars are the standard deviation of the measurement. The experimental temperature was 22.2 °C, the driving magnetic field strength was 0.40 A/m and the frequency range was from 20 Hz to 200 Hz.

The imaginary part of the permeability was corrected using the obtained wire resistance. The measured complex permeability of ferrite samples are shown in Fig. 5. As shown in Fig. 5, the trend of the imaginary part of permeability after correction agrees well with the nominal value. If the wire resistance was ignored, the measured value of the imaginary part would be two orders of magnitude larger than the nominal value. This indicates that this method effectively reduces the measurement error for the imaginary permeability at low frequency.

These four ferrite samples were measured using the same method during several different driving fields from 0.40 A/m to 1.10 A/m. The initial permeability of the ferrites were obtained by extrapolating the permeability to the zero driving field. Fig. 6 and Fig. 7 show the real part of permeability and the imaginary part of permeability response function for different magnetic field strengths, for which the data were fitted to (5). The fitting results are in good agreement with the nominal value in consideration of the temperature effect. Table 2 shows the fitting results for the complex permeability at zero driving field.

D. CALCULATION OF MAGNETIC NOISE AND SHIELDING FACTOR

Two cylindrical magnetic shields respectively were developed with several ferrite annuli of PC40 and PC47 materials. The cylindrical ferrite shields made of PC40 ferrite annuli is shown in Fig. 8, The diameter of the shield is 133 mm, and the thickness of the shield wall is 13 mm. The total length of the shield is 225 mm. After obtaining the initial complex permeability, the magnetic noise of the ferrite shield can be estimated. The intrinsic magnetic noise of magnetic shield can be divided into hysteresis noise and eddy-current noise at low frequency [2], [5]. For ferrite materials, the magnetic

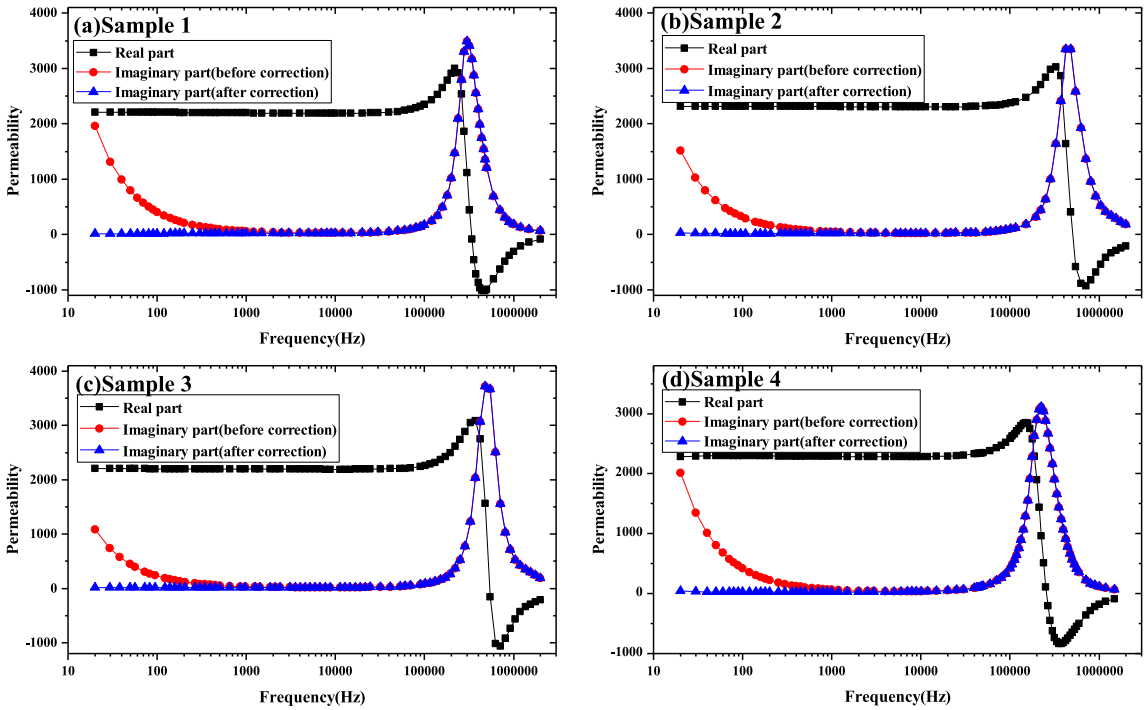

FIGURE 5. The experimental result of the real part (black squares), the imaginary part before eliminating the measurement error (red circles) and the imaginary part after eliminating the measurement error (blue triangle) of the complex permeability: (a) Sample 1; (b) Sample 2; (c) Sample 3; (d) Sample 4. The experimental temperature was 22.2 °C and the driving magnetic field strength was 0.40 A/m.

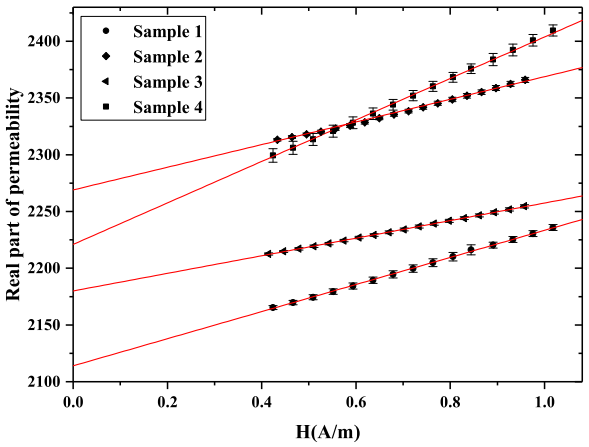

FIGURE 6. Experimental results of Sample 1 (black circles), Sample 2 (black rhombus), Sample 3 (black triangle) and Sample 4 (black squares) for the real part of permeability, fitted to (5) (red line). The error bars are the standard deviation of the measurement. The experimental temperature was 22.2 °C and the frequency range was from 20 Hz to 200 Hz.

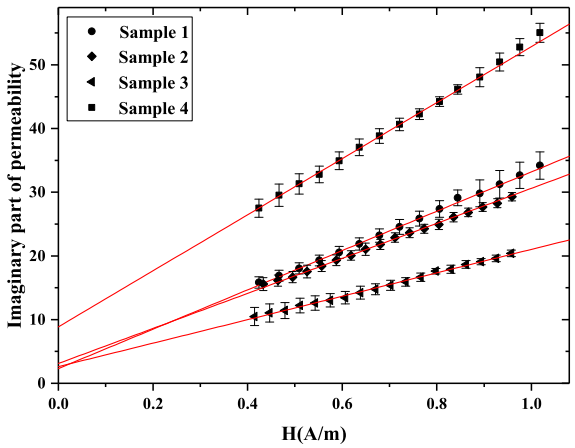

FIGURE 7. Experiment results of Sample 1 (black circles), Sample 2 (black rhombus), Sample 3 (black triangle) and Sample 4 (black squares) for the imaginary part of permeability, fitted to (5) (red line). The error bars are the standard deviation of the measurement. The experimental temperature was 22.2 °C and the frequency range was from 20 Hz to 200 Hz.

noise due to eddy-current noise is much smaller than that due to magnetic hysteresis noise. Hence, the magnetic noise of a ferrite shield, which is approximated to an infinitely long, cylindrical shield, can be described as [5]:

$$\delta B_{magn} = \frac{0.26}{r\sqrt{t}}\sqrt{\frac{4kT\mu_0\mu''}{\omega\mu'^2}} \tag{6}$$

where r and t are the inner radius and the thickness of the wall of the shield, k is the Boltzmann constant, and T is the operation temperature.

With the exception of the magnetic noise, the low-frequency shielding factor of the ferrite shields can be calculated using their permeability. The transverse shielding factor of a cylindrical shield can be described as [12]:

$$S_t = \frac{1}{4}\mu'\left(1 - \frac{(D-2t)^2}{D^2}\right) + \frac{1}{2}\left(1 + \frac{(D-2t)^2}{D^2}\right) \tag{7}$$

FIGURE 8. Cylindrical ferrite shields made of PC40 ferrite annuli.

TABLE 2. Measured initial complex permeability of PC40 and PC47 at low frequency, expected magnetic hysteresis noise, and expected shielding factor of the ferrite shield.

Material	μ'	μ''	$\delta B_{\text{magn}}(\text{fT}\cdot\text{Hz}^{-1/2})$	S_{t}	S_{a}
PC40(Sample 1)	2114	2.56	\	\	\
PC40(Sample 2)	2269	3.12	\	\	\
PC40(Sample 3)	2180	2.62	\	\	\
PC40(average)	2188	2.77	$1.80\cdot f^{-1/2}$	193.8	39.7
PC47(Sample 4)	2221	8.86	$3.16\cdot f^{-1/2}$	196.7	40.3

and the axial shielding factor of a cylindrical shield is [11]:

$$S_a = \frac{\left(\frac{4N\mu' t}{D} + 1\right)}{\left(1 + \frac{D}{2L}\right)} \tag{8}$$

where D is the diameter of the shield, L is the length of the shield, and N is the demagnetization factor for an ellipsoid with the dimensional ratio $p = L/D$:

$$N = \left[\frac{1}{(p^2-1)}\right]\left\{\frac{p}{(p^2-1)^{\frac{1}{2}}\ln\left[p+(p^2-1)^{\frac{1}{2}}\right]} - 1\right\} \tag{9}$$

Table 2 shows the calculated magnetic noise and shielding factor of these shields. The real parts of complex permeability of PC40 and PC47 are close so that the shielding factors are similar. However, there is a big difference of the imaginary part between the two materials which causes the difference of the magnetic hysteresis noise. The results indicate that the shield made of PC40 material has the lower magnetic hysteresis noise.

IV. CONCLUSION

In summary, we have propose an improved coil method of measuring the complex permeability of the ferrite annulus for low-noise magnetic shields which especially aims at low frequency (<200Hz). The measurement error of the conventional coil method was analyzed. The result of analysis indicates that the resistance of the wire is the primary cause for the significant measurement error of the complex permeability at low frequency, and can be identified and eliminated using our method. The ferrite annuli made of PC40 and PC47 materials are measured using this method. The experiment results demonstrate that the improved method effectively eliminates the measurement error for the imaginary permeability at low frequency and the measurement accuracy has improved two orders of magnitude. On the basis of the low-frequency complex permeability extrapolated to zero-field limit, both the magnetic hysteresis noise and the shielding factor of the cylindrical ferrite shields made of several ferrite annuli are calculated. The calculation results indicate that the PC40 shield has the lower magnetic hysteresis noise with the same size. This study can help select ferrite materials and estimate the performance for low-noise magnetic shield.

REFERENCES

[1] A. Mager, "Magnetic shields," *IEEE Trans. Magn.*, vol. MAG-6, no. 1, pp. 67–75, Mar. 1970.
[2] S.-K. Lee and M. V. Romalis, "Calculation of magnetic field noise from high-permeability magnetic shields and conducting objects with simple geometry," *J. Appl. Phys.*, vol. 103, no. 8, 2008, Art. no. 084904.
[3] J. C. Allred, R. N. Lyman, T. W. Kornack, and M. V. Romalis, "High-sensitivity atomic magnetometer unaffected by spin-exchange relaxation," *Phys. Rev. Lett.*, vol. 89, no. 13, Sep. 2002, Art. no. 130801.
[4] I. K. Kominis, T. W. Kornack, J. C. Allred, and M. V. Romalis, "A subfemtotesla multichannel atomic magnetometer," *Nature*, vol. 422, pp. 596–599, Apr. 2003.
[5] T. W. Kornack, S. J. Smullin, S.-K. Lee, and M. V. Romalis, "A low-noise ferrite magnetic shield," *Appl. Phys. Lett.*, vol. 90, May 2007, Art. no. 223501.
[6] M. C. D. Tayler, T. Theis, T. F. Sjolander, J. W. Blanchard, A. Kentner, S. Pustelny, A. Pines, and D. Budker, "Invited review article: Instrumentation for nuclear magnetic resonance in zero and ultralow magnetic field," *Rev. Sci. Instrum.*, vol. 88, no. 9, 2017, Art. no. 091101.
[7] D. Bevan, M. Bulatowicz, P. Clark, J. Flicker, R. Griffith, M. Larsen, M. Luengo-Kovac, J. Pavell, A. Rothballer, D. Sakaida, E. Burke, J. Campero, B. Ehrsam, and E. G. Morrison, "Nuclear magnetic resonance gyroscope: Developing a primary rotation sensor," in *Proc. IEEE INERTIAL*, Mar. 2018, pp. 1–2.
[8] H. B. Dang, A. C. Maloof, and M. V. Romalis, "Ultrahigh sensitivity magnetic field and magnetization measurements with an atomic magnetometer," *Appl. Phys. Lett.*, vol. 97, no. 15, Oct. 2010, Art. no. 151110.
[9] I. Savukov, Y. J. Kim, V. Shah, and M. G. Boshier, "High-sensitivity operation of single-beam optically pumped magnetometer in a kHz frequency range," *Meas. Sci. Technol.*, vol. 28, no. 3, 2017, Art. no. 035104.
[10] Y. Chen, W. Quan, S. Zou, Y. Lu, L. Duan, Y. Li, H. Zhang, M. Ding, and J. Fang, "Spin exchange broadening of magnetic resonance lines in a high-sensitivity rotating K-Rb-^{21}Ne co-magnetometer," *Sci. Rep.*, vol. 6, Nov. 2016, Art. no. 36547.
[11] A. Mager, "Magnetic shielding efficiencies of cylindrical shells with axis parallel to the field," *J. Appl. Phys.*, vol. 39, no. 3, p. 1914, 1968.
[12] A. K. Thomas, "Magnetic shielded enclosure design in the DC and VLF region," *IEEE Trans. Electromagn. Compat.*, vol. EMC-10, no. 1, pp. 142–152, Mar. 1968.
[13] D. K. Ghodgaonkar, V. V. Varadan, and V. K. Varadan, "Free-space measurement of complex permittivity and complex permeability of magnetic materials at microwave frequencies," *IEEE Trans. Instrum. Meas.*, vol. 39, no. 2, pp. 387–394, Apr. 1990.
[14] V. Bekker, K. Seemann, and H. Leiste, "A new strip line broad-band measurement evaluation for determining the complex permeability of thin ferromagnetic films," *J. Magn. Magn. Mater.*, vol. 270, no. 3, pp. 327–332, Apr. 2004.
[15] A. Vepsäläinen, K. Chalapat, and G. S. Paraoanu, "Measuring the microwave magnetic permeability of small samples using the short-circuit transmission line method," *IEEE Trans. Instrum. Meas.*, vol. 62, no. 9, pp. 2503–2510, Sep. 2013.
[16] A. K. Jha and M. J. Akhtar, "An improved rectangular cavity approach for measurement of complex permeability of materials," *IEEE Trans. Instrum. Meas.*, vol. 64, no. 4, pp. 995–1003, Apr. 2015.
[17] M. H. Hosseini, H. Heidar, and M. H. Shams, "Wideband nondestructive measurement of complex permittivity and permeability using coupled coaxial probes," *IEEE Trans. Instrum. Meas.*, vol. 66, no. 1, pp. 148–157, Jan. 2017.

[18] T. Tsutaoka, M. Ueshima, T. Tokunaga, and T. Nakamura, "Frequency dispersion and temperature variation of complex permeability of Ni–Zn ferrite composite materials," *J. Appl. Phys.*, vol. 78, no. 6, pp. 3983–3991, 1995.
[19] T. Nakamura and K. Hatakeyama, "Complex permeability of polycrystalline hexagonal ferrites," *IEEE Trans. Magn.*, vol. 36, no. 5, pp. 3415–3417, Sep. 2000.
[20] T. Tsutaoka, "Frequency dispersion of complex permeability in Mn–Zn and Ni–Zn spinel ferrites and their composite materials," *J. Appl. Phys.*, vol. 93, no. 5, pp. 2789–2796, 2003.
[21] J. Shenhui and J. Quanxing, "An alternative method to determine the initial permeability of ferrite core using network analyzer," *IEEE Trans. Electromagn. Compat.*, vol. 47, no. 3, pp. 651–657, Aug. 2005.
[22] *Solutions for Measuring Permittivity and Permeability With LCR Meters and Impedance Analyzers*, Keysight, Santa Rosa, CA, USA, 2017.
[23] K. Klopfer, U. Niedermayer, H. Klingbeil, W. Ackermann, H. G. König, and T. Weiland, "Measurement of the magnetic material properties for ferrite-loaded cavities," *Phys. Rev. Accel. Beams*, vol. 18, no. 1, 2015, Art. no. 010101.
[24] *Cores Made of Soft Magnetic Materials—Measuring Methods—Part 2: Magnetic Properties at Low Excitation Level*, document IEC 62044-2, 2005.
[25] *Mn–Zn Ferrite Material Characteristics*, TDK, Tokyo, Japan, 2019.
[26] T. M. Baynes, G. J. Russell, and A. Bailey, "Comparison of stepwise demagnetization techniques," *IEEE Trans. Magn.*, vol. 38, no. 4, pp. 1753–1758, Jul. 2002.
[27] X. Ke, J. Li, C. Nisoli, Paul E. Lammert, W. McConville, R. F. Wang, V. H. Crespi, and P. Schiffer, "Energy minimization and AC demagnetization in a nanomagnet array," *Phys. Rev. Lett.*, vol. 101, no. 3, 2008, Art. no. 037205.

KE YANG received the B.E. degree in information engineering from Beihang University, Beijing, China, in 2016, where he is currently pursuing the Ph.D. degree. His current research interests include the atomic magnetometer and magnetic shielding technology.

JIXI LU received the Ph.D. degree in measurement technology and instruments from Beihang University, Beijing, China, in 2016, where he is currently a Lecturer with the School of Instrumentation and Optoelectronic Engineering. His research interests include atomic magnetometer and electronic-optical detection technology.

MING DING received the Ph.D. degree in optoelectronics from the Optical Fiber Nanowires and Related Devices Group, Optoelectronics Research Centre, University of Southampton, Southampton, U.K., in 2013. She is currently a Professor with the School of Instrumentation and Optoelectronic Engineering, Beihang University, Beijing, China. Her current research interests include atomic magnetometers, micro- and nanoresonators, and micro- and nanofiber.

JUNPENG ZHAO received the B.E. degree in measurement and control technology and instrumentation from the Hebei University of Technology, Tianjin, China, in 2015. He is currently pursuing the Ph.D. degree with Beihang University, Beijing, China. His research interest includes optically pumped atomic magnetometers.

DANYUE MA received the B.E. degree in mechanical engineering and automation from the Beijing University of Technology, Beijing, China, in 2016. She is currently pursuing the Ph.D. degree with Beihang University, Beijing. Her current research interest includes magnetic shield design.

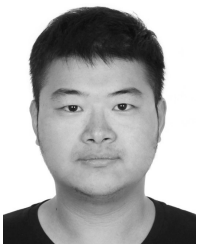

YANG LI received the B.S. degree in applied physics from Beihang University, Beijing, China, in 2011, where he is currently pursuing the Ph.D. degree. His current research interest includes hybrid optical pumping atomic magnetometers.

BOZHENG XING received the B.E. degree in information engineering from Beihang University, Beijing, China, in 2017, where he is currently pursuing the Ph.D. degree. His current research interests include atomic magnetometers and optical detection.

BANGCHENG HAN received the Ph.D. degree in mechanical manufacture and automation from the Changchun Institute of Optics, Fine Mechanics and Physics, Chinese Academy of Sciences, Changchun, China, in 2004. He is currently a Professor with the School of Instrumentation and Optoelectronic Engineering, Beihang University, Beijing, China. His research interests include mechatronics, magnetic suspension technology, attitude control actuator of spacecraft, and precision measurement.

JIANCHENG FANG received the Ph.D. degree in mechanical engineering from Southeast University, Nanjing, China, in 1996. He is currently a Professor with the School of Instrumentation and Optoelectronic Engineering, Beihang University, Beijing, China, where he is also the Vice President. He was inducted as a member of the Chinese Academy of Sciences, in 2015. His current research interests include precise instrument and measurement, inertial navigation, and integrated navigation technologies of aerial vehicles.